Article

On the Dynamic Robustness of a Non-Endoreversible Engine Working in Different Operation Regimes

Norma Sanchez-Salas [1,*], **Juan C. Chimal-Eguia** [2,3] **and Florencio Guzman-Aguilar** [4]

[1] Departamento de Física, Escuela Superior de Física y Matemáticas del IPN, Edif. 9 U.P. Zacatenco CP 07738, D.F., Mexico

[2] Centro de Investigación en Computación del I.P.N., Av. Juan de Dios Bátiz s/n U.P. Zacatenco CP 07738, D.F., Mexico; E-Mail: jchimale@ipn.mx

[3] Centre for Mathematical Biology, Department of Mathematics and Statistics Sciences, University of Alberta, Edmonton, Alberta T6G 2E1, Canada

[4] Departamento de Formación Básica, Escuela Superior de Cómputo del IPN, Av. Miguel Bernal Esq. Juan de Dios Bátiz U.P. Zacatenco CP 07738, D.F., Mexico; E-Mail: fguzmana@ipn.mx

[*] Author to whom correspondence should be addressed; E-Mail: norma@esfm.ipn.mx; Tel.: +52-572-9600 ext. 55017; Fax: +52-572-9600 ext. 55015.

Abstract: In this work, we focused mainly in the analysis of stability of a non-endoreversible Curzon-Ahlborn engine working in an ecological regime. For comparison purposes we also include the Maximum Efficient Power (MEP) regime taking into account the engine time delays. When the system's dynamic stability is compared with its thermodynamics properties (efficiency and power output), we find that the temperature ratio $\tau = T_1/T_2$ represents a trade-off between stability and energetic properties. When we take the non-endoreversible case, τ can increases to values greater than R (where R is the non-endoreversible parameter) but not greater than one. We reformulate an important difference between this case and the other two, Maximum Power (MP) and MEP regime, in which $\tau = R$. Finally, we demonstrated that the total time delay does not destabilize the steady state of system. It does not seem to play a role in the dynamic thermodynamic property trade-off.

1. Introduction

It is well known that the universal validity of the maximum Carnot efficiency $\eta_C = 1 - T_2/T_1 \equiv 1 - \tau$ for any reversible heat engine operating between reservoirs at temperatures T_1 and T_2 ($T_1 > T_2$) has little practical relevance since it applies to zero-power output heat devices. On the contrary, real heat engines work at nonzero power and evolve along irreversible paths coming from finite-time and finite-size unavoidable constraints. In 1975, Curzon and Ahlborn [1] introduced a Carnot-like thermal engine in which there was no thermal equilibrium between the working fluid and the thermal reservoirs at the isothermal branches of the cycle. Curzon and Ahlborn (CA) demonstrated that such an engine delivers nonzero power, a positive entropy production and has more realistic efficiency than that the Carnot engine.

The efficiency of a CA engine in the performance of maximum power is given by $\eta_{CA} = 1 - \sqrt{\frac{T_2}{T_1}}$. We can thus conclude that the CA engine is a better approximation to real engines than the Carnot engine. This seminal paper led to the establishment of a new brand of irreversible thermodynamics, known as finite-time thermodynamics (FTT), which has been developed during last decades [2–11].

Most of the studies of FFT systems have been concerned with their steady-state energetic properties, which are important from the point of view of design. The steady-state operation regime ought to have optimal thermodynamic properties: high power output, also high efficiency, low entropy production, etc. In some models heat leak [12–14] and internal irreversibilities [15,16] are considered. An irreversible model with heat resistance, heat leakage and internal irreversibility with different heat transfer laws was studied [17–20]. On the other hand, only a few of these studies have dealt with the system's dynamic properties, such as the response to a noisy perturbation or the stability of the system's steady state. The robustness of a system can be manifested itself in one of two different ways: either the system returns to its current dynamics attractor after perturbation, or moves to a different attractor that maintains the system's function.

Although both dynamics robustness and energetic properties should be taken into account when building an energy-converting systems, there have been a few studies analyzing both. Santillán *et al.* [21] studied an endoreversible CA engine working at maximum power regime and found that a good design implies a trade-off between dynamics robustness and optimal thermodynamic properties. Afterwards, Guzmán *et al.* [22,23] extended this study considering different heat transfer laws. Recently, an interesting study was presented where dynamic stability versus thermodynamic performance in a Brownian motor were analyzed [24].

One of central questions addressed in FFT is to identify optimal procedures for different objective functions. Originally Curzon and Ahlborn proposed to optimize the power output but some other different functions had been proposed. One of this criteria introduced in 1991 by Angulo [25] was called the ecological function, which is the main objective function, given by:

$$E = P - T_2\sigma \qquad (1)$$

where P is the power output of the cycle, σ is the total entropy production (system plus the surroundings) per cycle, and T_2 is the temperature of the cold reservoir. Several papers of ecological performance for irreversible engines have been written [26–31]. When we use this criteria of optimization, the power output satisfies $P_{E_{max}} \approx 3/4 P_{P_{max}}$, and the entropy production is $\sigma_{E_{max}} \approx \sigma_{P_{max}}/4$. These were the

reasons that it was called ecological function. Another important property of optimal ecological regime is that the efficiency can be expressed as,
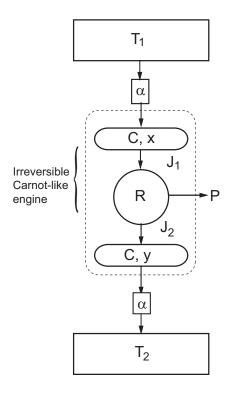
$$\eta_E \approx \frac{1}{2}(\eta_C + \eta_{CA}) \tag{2}$$

This paper presents an analysis of the dynamic robustness of a non-endoreversible thermal engine when it operates at two different operation regimes, *i.e.*, maximum ecological regime and maximum efficient power [32], instead of the power-like regime used by Paéz-Hernández *et al.* [33], in order to obtain certain qualitative relations between the dynamical stability and the thermodynamical properties at these different operation regimes. The paper is organized as follows: Section 2 presents the properties of the non-endoreversible Curzon-Ahlborn engine in steady-state condition. Section 3 presents a brief general analysis of the stability theory when we have fixed points. Section 4 presents the stability analysis of the non-endoreversible Curzon-Ahlborn engine under small perturbations. In Sections 5 and 6 we discuss some numerical results and Section 7 presents some concluding remarks.

2. The Steady-State Properties of a Non-Endoreversible Curzon-Ahlborn Engine

In Figure 1, a schematic diagram of a non-endoreversible Curzon-Ahlborn engine is presented. This model is a Carnot-like engine but it is modified. It works on irreversible cycles and exchanges heat irreversibly with external thermal reservoirs at temperatures T_1 and T_2, respectively, at the hot branch and the cold one (*i.e.*, $T_2 > T_1$). In the steady state, working temperatures are $\bar{x}$ and $\bar{y}$, where $T_1 > \bar{x} > \bar{y} > T_2$ (hereinafter overbar is used to denote steady-state variables). The flows of heat from T_1 to $\bar{x}$ and from $\bar{y}$ to T_2 are modeled by Newton heat transfer laws, with a heat conductance denoted by α.

Figure 1. Diagram of a non-endoreversible Curzon-Ahlborn engine.

Thus,

$$\bar{J}_1 = \alpha(T_1 - \bar{x}) \tag{3}$$

$$\bar{J}_2 = \alpha(\bar{y} - T_2) \tag{4}$$

The inner part of engine works in an irreversible cycle, then, from Clausius theorem

$$\frac{\bar{J}_1}{\bar{x}} - \frac{\bar{J}_2}{\bar{y}} < 0 \tag{5}$$

this expression can be re-written as equality as follows:

$$\frac{\bar{J}_1}{\bar{x}} = R\frac{\bar{J}_2}{\bar{y}} \tag{6}$$

where $0 \leq R \leq 1$ is a constant that measures the level of internal irreversibility; the smaller the value of R, the more irreversible the inner Carnot-like engine.

The system's steady-state power output can be written as,

$$\bar{P} = \bar{J}_1 - \bar{J}_2 \tag{7}$$

and the efficiency as,

$$\bar{\eta} = \frac{\bar{P}}{\bar{J}_1} = 1 - \frac{\bar{J}_2}{\bar{J}_1} \tag{8}$$

Solving for $\bar{x}$ and $\bar{y}$ from Equations (3) (4), (6) and (8) we get,

$$\bar{x} = \frac{T_1}{R+1}\left(1 + \frac{\tau}{1-\bar{\eta}}\right) \tag{9}$$

$$\bar{y} = \frac{RT_1}{R+1}\left(1 + \frac{\tau}{1-\bar{\eta}}\right)(1-\bar{\eta}) \tag{10}$$

where $\tau = T_2/T_1$.

On the other hand, the efficiency of a non-endoreversible Curzon-Ahlborn engine working at maximum ecological conditions is [34],

$$\bar{\eta}_{ME} = 1 - \sqrt{\frac{\tau(\tau+1)}{2R}} \tag{11}$$

By substitution of this expression into Equations (9), (10) we found,

$$\bar{x} = \frac{T_1}{R+1}\left(1 + \sqrt{\frac{2R\tau}{\tau+1}}\right) \tag{12}$$

$$\bar{y} = \frac{T_1}{R+1}\sqrt{R\tau}\left(\sqrt{\frac{\tau+1}{2}} + \sqrt{R\tau}\right) \tag{13}$$

Now, by solving for T_1 and T_2 from Equations (12) and (13) we obtain,

$$T_1 = \frac{(R+1)\bar{x}}{2}\left(\frac{R\bar{x} - 2\bar{y} + \sqrt{R}\sqrt{R\bar{x}^2 + 8\bar{y}^2}}{R(\bar{x} + 2\bar{y}) - \bar{y}}\right) \tag{14}$$

$$T_2 = 4(R+1)\left(\frac{\bar{y}^2}{R(\bar{x} + 4\bar{y}) + \sqrt{R}\sqrt{R\bar{x}^2 + 8\bar{y}^2}}\right) \tag{15}$$

By combining Equations (3), (8), (11) and (12), it is possible write the system's steady-state power output as,

$$\bar{P} = \frac{\alpha T_1 R}{R+1}\left(1 - \frac{\sqrt{2\tau}}{\sqrt{R}\sqrt{\tau+1}}\right)\left(1 - \sqrt{\frac{\tau(\tau+1)}{2R}}\right) \tag{16}$$

Finally, if Equations (14) and (15) are substitute in Equation (16), we get,

$$\bar{P} = \frac{(R\bar{x} - \bar{y})\left(R\bar{x} - 2\bar{y} + \sqrt{R}\sqrt{R\bar{x}^2 + 8\bar{y}^2}\right)\left(-2\sqrt{2}\bar{y} + \sqrt{R}\sqrt{R\bar{x}^2 + 4\bar{y}^2 + \sqrt{R}\bar{x}\sqrt{R\bar{x}^2 + 8\bar{y}^2}}\right)}{2\sqrt{R}(R(\bar{x} + 2\bar{y}) - \bar{y})\sqrt{R\bar{x}^2 + 4\bar{y}^2 + \sqrt{R}\bar{x}\sqrt{R\bar{x}^2 + 8\bar{y}^2}}} \tag{17}$$

Power output in terms of $\bar{x}$ and $\bar{y}$, recall that these are not independent variables.

3. Dynamic Equations of a Non-Endoreversible Curzon-Ahlborn Engine

Consider again the endoreversible Curzon-Ahlborn engine of Figure 1. Now the reservoirs x and y are not real heat reservoirs but macroscopic objects with heat capacity C, and their temperatures change according to the following differential equations:

$$\frac{dx}{dt} = \frac{1}{C}(\alpha(T_1 - x) - J_1(x, y_{\pi/2})) \tag{18}$$

$$\frac{dy}{dt} = \frac{1}{C}(J_2(x_{\pi/2}, y) - \alpha(y - T_2)) \tag{19}$$

Both of these derivatives are null when x, y, J_1 and J_2 take their steady-state values. $x_{\pi/2}$ and $y_{\pi/2}$ denote variables x and y delayed a time $\pi/2$, respectively, and π is the period of non-endoreversible Curzon-Ahlborn engine cycles. These time delays are included because each isothermal branch cannot have information of the other branch immediately but only have the value it had half a cycle ago. Equations (18) and (19) are only possible for huge time scales, as compared to the thermal engine period. That is because x and y are the respective temperatures of the working fluid at hot and cold isotherms of the inner Carnot cycle, and they are not well defined at all times. In spite of that, if π is brief according to cycle time scale, the problem can be dismissed by assuming that x and y take constant values along the whole cycle.

On the other hand, Equation (7) comes from first law of thermodynamics while Equation (8) is the definition of efficiency. Therefore, they can be assumed valid out of the steady state. Relation (6) is more complicated because all internal irreversibilities are included in the factor R and these in principle are strongly non-linear, often dependent on temperature derivatives. But the purpose of this work is only to qualitative analyze and understand the intrinsic properties of machines in agreement with structural theory [35]. Then, at a first approximation we assume that Equation (6) is also valid out of the steady state. Based on this hypothesis it is possible to write the following expressions for J_1 and J_2

$$J_1 = \frac{Rx}{Rx - y}P \tag{20}$$

$$J_2 = \frac{Ry}{Rx - y}P \tag{21}$$

Also, it is possible to consider that P, out of but close to steady state, depends on x and y in the same way as $\bar{P}$ depends on $\bar{x}$ and $\bar{y}$; that is

$$P = \frac{(Rx - y)\left(Rx - 2y + \sqrt{R}\sqrt{Rx^2 + 8y^2}\right)\left(-2\sqrt{2}y + \sqrt{R}\sqrt{Rx^2 + 4y^2 + \sqrt{R}x\sqrt{Rx^2 + 8y^2}}\right)}{2\sqrt{R}(R(x + 2y) - y)\sqrt{Rx^2 + 4y^2 + \sqrt{R}x\sqrt{Rx^2 + 8y^2}}}$$

(22)

Equation (22) represents the regime defined as the maximum-ecological-like regime.

4. Local Stability Analysis

Let $f(x, y)$ and $g(x, y)$ be defined as,

$$\frac{dx}{dt} = f(x, y)$$

(23)

$$\frac{dy}{dt} = g(x, y)$$

(24)

with

$$f(x, y) = \frac{\alpha}{C}\left[T_1 - x - Rx\frac{\left(Rx - 2y + \sqrt{R}\sqrt{Rx^2 + 8y^2}\right)\left(\sqrt{R}\sqrt{Rx^2 + 4y^2 + \sqrt{R}x\sqrt{Rx^2 + 8y^2}}\right)}{2\sqrt{R}x(R(x + 2y) - y)\sqrt{Rx^2 + 4y^2 + \sqrt{R}x\sqrt{Rx^2 + 8y^2}}}\right]$$

(25)

$$g(x, y) = \frac{\alpha}{C}\left[T_2 - y + y\frac{\left(Rx - 2y + \sqrt{R}\sqrt{Rx^2 + 8y^2}\right)\left(\sqrt{R}\sqrt{Rx^2 + 4y^2 + \sqrt{R}x\sqrt{Rx^2 + 8y^2}}\right)}{2\sqrt{R}x(R(x + 2y) - y)\sqrt{Rx^2 + 4y^2 + \sqrt{R}x\sqrt{Rx^2 + 8y^2}}}\right]$$

(26)

The steady-state solutions $\bar{x}$ and $\bar{y}$ are couples $(\bar{x}, \bar{y})$ that simultaneously satisfy $f(\bar{x}, \bar{y}) = 0$ and $g(\bar{x}, \bar{y}) = 0$.

Following Strogatz [36], the steady-state local stability is determined by the eigenvalues of the Jacobian matrix:

$$J = \begin{pmatrix} f_x & f_y \\ g_x & g_y \end{pmatrix}$$

(27)

where

$$f_x = \frac{\partial f}{\partial x}\big|_{\bar{x}, \bar{y}}$$

(28)

$$f_y = \frac{\partial f}{\partial y}\big|_{\bar{x}, \bar{y}}$$

(29)

$$g_x = \frac{\partial g}{\partial x}\big|_{\bar{x}, \bar{y}}$$

(30)

$$g_y = \frac{\partial g}{\partial y}\big|_{\bar{x}, \bar{y}}$$

(31)

Let λ_1 and λ_2 denote the Jacobian matrix eigenvalues, and let $\vec{v}_1$ and $\vec{v}_2$ be their respective eigenvectors. The temporal evolution of small perturbations from steady state, δx and δy, is given by

$$\begin{pmatrix} \delta_x \\ \delta_x \end{pmatrix} = c_1 \vec{v}_1 exp(\lambda_1 t) + c_2 \vec{v}_2 exp(\lambda_2 t) \tag{32}$$

where, c_1 and c_2 are constants to be determined from initial conditions. Then, it follows from Equation (32) that the steady state is stable if both eigenvalues have negative real parts. In particular, if the two eigenvalues are real and negative, the functions δx and δy converge to zero monotonically. In this case, we call the steady state a stable node.

Let Ξ and Δ denote the trace and the determinant of the Jacobian matrix respectively, *i.e.*,

$$\begin{aligned} \Xi(R,\tau) &= f_x + g_y \\ \Delta(R,\tau) &= f_x g_y - f_x g_y \end{aligned}$$

The eigenvalues can then be calculated as

$$\lambda_1(R,\tau) = \frac{1}{2}\left(\Xi + \sqrt{\Xi^2 - 4\Delta}\right) \tag{33}$$

$$\lambda_2(R,\tau) = \frac{1}{2}\left(\Xi - \sqrt{\Xi^2 - 4\Delta}\right) \tag{34}$$

Since R and τ are positive constants $f_x, g_y < 0$ and $f_y, g_x > 0$. Thus further implies that $\Xi < 0$, $\Delta > 0$ and $\Xi^2 > 4\Delta$. It follows then from Equations (33) and (34) that both λ_1 and λ_2 are negative real numbers and the system steady state is a stable node.

5. Dynamic Robustness *vs.* Power and Efficiency

The efficiency and the power output, in the steady state, are written in Equations (11) and (16), as functions of $\tau = T_2/T_1$ and R, for a non-endoreversible Curzon-Ahlborn engine working in the maximum ecological-like regime. In Figure 2, we depicted the thermal efficiency as a function of τ for three different optimization criteria, namely, Maximum Power (MP), Maximum Ecological Regime (ME), and Maximum Efficient Power (MEP) [32]. In each case, we can notice that all are decreasing functions of τ for every value of R. It is important to mention that the maximum power case and the maximum efficient power case has a root for $\tau = R$. However, in the maximum ecological regime, $\eta = 0$ happens at $\tau > R$. In Figure 3 we graph τ as a function of R, when $\eta = 0$, for different regimes. It is clear that for the maximum power case and the maximum efficient power, the functional relation between τ and R is linear, and in the other cases the relation is not. This is a notable difference between the maximum ecological regime and the other two, in the sense that the irreversibilities represented by R in the first case reduces the parameter τ (and consequently the stability) in a linear fashion but not in the last regime.

In other words, in the maximum power case and the maximum efficient power, the irreversibilities play exactly the same role of τ because of its functional relation. Consequently, if we accept a trade-off between the stability and the parameter τ, the inclusion of irreversibilities in the engine only reduces the stability's trade-off in the same manner as we increase or decrease the irreversibilities. However, this

is not the case in the ecological regime, in which if we decrease the irreversibilities of the engine, the parameter τ and the stability do not decrease as significantly.

Figure 2. Plots of power output normalized and efficiency *vs.* τ for $R = 0.5$ for MP, ME, MEP regime.
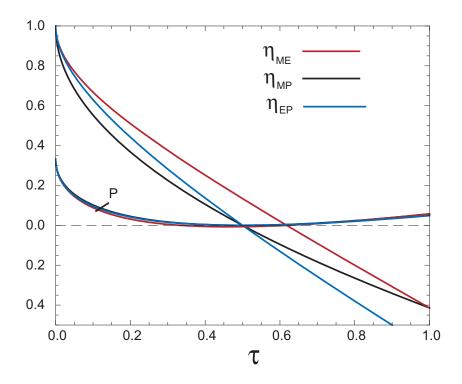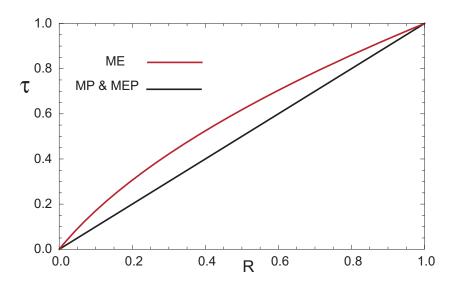

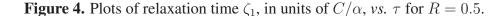**Figure 3.** Plots τ *vs.* R when $\eta = 0$.

We can also say that the energetic properties of our model decay as τ increases in the maximum-ecological regime as well as in the other two other regimes. In addition, the parameter τ can only increase up to $\tau^* \approx 0.62$ for the maximum ecological regime when the parameter $R = 0.5$. Greater values of τ gives non-physical values of $\bar{\eta}$ and $\bar{P}$. In the other two cases τ can only increase up to $\tau = R = 0.5$.

Also in a previous section we showed that both eigenvalues of the Jacobian matrix are real and negative for all values of τ and R in $[0, 1]$, which means that the engine steady state is a stable node and allows us to define relaxation time $\varsigma_i = -1/\lambda_i$, $i = 1, 2$. The time evolution of given perturbations from the steady state is often determined by both relaxation times, but the perturbation long-time behavior is managed by the longest relaxation time.

In Figures 4 and 5, the relaxation time ς_1 and ς_2 are plotted versus τ for $R = 0.5$ and for the three different optimization criteria. The plot shows that for every regime of operation $\varsigma_1 > \varsigma_2$ for all values of τ, both relaxation times have a minimum in the interval of $\tau \in [0, 1]$, in all the criteria.
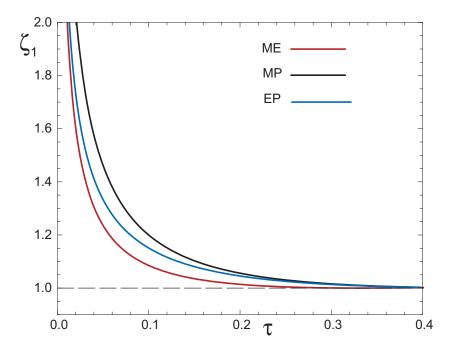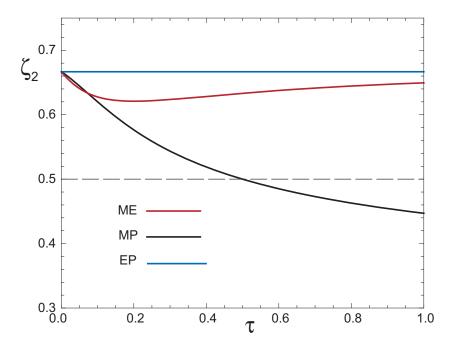
Figure 4. Plots of relaxation time ζ_1, in units of C/α, *vs.* τ for $R = 0.5$.

Figure 5. Plots of relaxation time ζ_2, in units of C/α, vs. τ for $R = 0.5$.

As mentioned previously, the long-term behavior of perturbation from the steady state is dominated by the longest relaxation time, ς_1, for all the cases. Thus, the minimum ς_1 value represents an optimal dynamic state in which the system stability is maximal. It was followed from Figure 2 that as τ increase, the thermodynamic properties degraded. Also, from Figure 4, relaxation times decrease as τ increases, thus improving the system stability. Then, τ represents a trade-off between healthy stability and better thermodynamic properties as power or efficiency.

6. Dynamic Effects of the Time Delays

Recall the systems of delay differential equations given by Equations (25) and (26). They can be written as

$$\frac{dx}{dt} = f(x, y_{\pi/2})$$
$$\frac{dy}{dt} = g(x_{\pi/2}, y)$$

Following the method of McDonald [37], the time course of small perturbations from the steady state is determined by a linear combinations of the next terms: $exp(\lambda_i t)$, $i = 1, 2, ...$ where λ_i are the solutions of the characteristic equation.

$$(f_x - \lambda)(g_y - \lambda) - f_y g_x exp(-\lambda \pi) = 0 \tag{35}$$

It is known that a common effect of time delay is to destabilize already stable steady state by inducing sustained oscillations. To analyze if it occurs, suppose that λ is imaginary ($\lambda = i\omega$) and substitute it into the characteristic equations, to obtain

$$(-A\omega^2 + B) + iD\omega = exp(-i\omega\pi) \tag{36}$$

with

$$A = \frac{1}{f_y g_x}$$
$$B = \frac{f_x g_y}{f_y g_x}$$
$$D = -\frac{f_x + g_y}{f_y g_x}$$

It is possible to show, from Equations (28–31), that $f_x, g_y < 0$, while $f_y, g_x > 0$. Consequently, A, B, and D are positive.

The left-hand side of Equation (36) determines the lower branch of a horizontal parabola in the complex plane. The position of parabola's vertex is in the point $(B, 0)$. On the other hand, the r.h.s. of Equation (36) is a unitary circle in the complex plane. The set points where these curves intersect correspond to values of ω and π where sustained oscillations arise because of a destabilization of the steady state, or vice versa. If both curves never intersect, the steady state cannot be moved from the balance by the delay π, not matter how long this is.

Now, set ρ and σ to be real variables along the real and imaginary axes, respectively, of the complex plane. In terms of these variables, the equation for the parabola can be expressed as,

$$\rho = B - \frac{A}{D^2}\sigma^2 \tag{37}$$

and the equation of circle as,

$$\rho^2 + \sigma^2 = 1 \tag{38}$$

To find the set of points where both curves intersect, we solve for σ in the Equation (37) and substitute into Equation (38), it renders

$$\rho^2 - \frac{D^2}{A}\rho + \frac{BD^2 - A}{A} = 0 \tag{39}$$

By solving above equation we get the real coordinates of the intersecting points. The corresponding imaginary coordinates can be calculated be means of Equation (38) as $\sigma = -\sqrt{1 - \rho^2}$. The solutions of Equation (39) are,

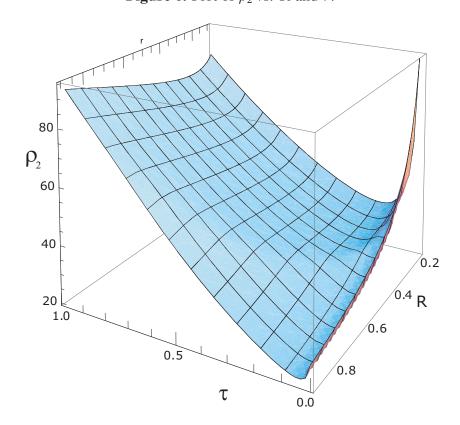$$\rho_1 = \frac{L}{2} + \frac{1}{2}\sqrt{L^2 - 4K} \tag{40}$$

and

$$\rho_2 = \frac{L}{2} - \frac{1}{2}\sqrt{L^2 - 4K} \tag{41}$$

where $L = D^2/A$ and $K = (BD^2 - A)/A$.

Before we have concluded that A and D are positive, so L is also positive and then $\rho_1 > \rho_2$. Finally in Figure 6, we show the plot ρ_2 in function of R and τ. It is worth mentioning that $\rho_2 > 20$ for all acceptable values of R and τ. Then the parabola, Equation (37), and circle, Equation (38), never intersect and non-endoreversible Curzon-Ahlborn engine at ecological regime cannot be destabilized by any time delay.

Figure 6. Plot of ρ_2 *vs.* R and τ.

7. Concluding Remarks

In this paper we have extended a previous work by Paez-Hernandez [33] and Santillan [21] and studied the local stability of an endoreversible Curzon-Ahlborn engine working in the ecological regime, with inclusion of the engine inherent time delays to account for internal irreversibilities. Besides, in order to compare the ecological and Maximum power regimes, we included a third criteria named Maximum efficient power.

Our results indicate that the only effect of internal irreversibilities is to decrease the range of physically allowed values of $\tau = T_2/T_1$. In an endoreversible engine, τ can vary from zero to one. However, in a non-endoreversible engine, τ depends on the value of R, where R is the parameter the measures the degree of internal irreversibilities; the shorter value of R, the more irreversible the inner Carnot-like engine.

In agreement with Santillan *et al.* [33], the stability of the non-endoreversible Curzon-Ahlborn engine strengthens as τ increases. However, an important difference between this regime and the maximum power regime used in Santillan's paper or the Maximum Efficient Power regime is that the parameter τ does not depend linearly on the parameter R.

The stability of the non-endoreversible Curzon-Ahlborn engine strengthens as τ increases. Conversely, the steady-state power output and efficiency decreases as τ increases. The system thermodynamical properties optimize at $\tau = 0$, but the stability is lost, given that the relaxation time ζ_1 diverges. On the other hand, both relaxation times minimize, so the system stability optimizes when τ reaches its upper bound, which at the same time is a function of the parameter R.

As a conclusion, the parameter τ represents a trade-off between stability strength and thermodynamic properties in a non-endoreversible Curzon-Ahlborn engine working in the ecological-power-like regime. However, the strength of τ depends on the relation between this parameter and the parameter R, and is determined by the operation regime used. This property could have an important consequence, because if we consider that the internal irreversibility affects the efficiency and stability of the engines, then it is important to take precautions to reduce internal irreversibility in the design of a heat engine working at MP (or Maximum efficient power) condition with respect to the ecological regime, since depending on its operation regime, the engine may have an increment in its stability.

The above conclusion is reinforced if we consider Figure 4, since we can observe that for the Maximum Power and the Maximum Efficient Power, the relaxation times for a specific τ are greater than the relaxation time for the Maximum Ecological Regime. This again enhanced the idea that for the Maximum Ecological Regime, we have better stability conditions than for the other two regimes. Once we have a small perturbation to the steady state, the time in which the engine at the ecological regime returns to the steady state is less than the other two. In other words, the operation regime plays a important role for the design of engines with better stability conditions. This is because, if we consider that the trade-off between dynamical properties and thermodynamic properties is driven by the parameter τ, which in turn is a function of the parameter R, then the operation regime determines whether the relation between τ and R is linear or not and consequently enhance the stability conditions.

Finally, we can say that time delays are present in many systems subject to dynamic regulation. In the non-endoreversible Curzon-Ahlborn engine, the inherent time delays are not capable of destabilizing

the steady state. Thus, they do not seem to play an important role in the trade-off between energetic and dynamic properties.

Acknowledgements

References

1. Curzon, F.; Ahlborn, B. Efficiency of a Carnot engine at maximum power output. *Am. J. Phys.* **1975**, *43*, 22–24.
2. De Vos, A. *Endoreversible Thermodynamics of Solar Energy Conversion*; Oxford University Press: New York, NY, USA, 1992.
3. Sieniutycs, S.; Salamon, P. *Finite-Time Thermodynamics and Thermoeconomics*; Taylor and Francis: New York, NY, USA, 1990.
4. Wu, C.; Chen, L.; Chen, J. *Recent Advances int Finite-Time Thermodynamics*; Nova Science Publishers: New York, NY, USA, 1999.
5. Bejan, A. *Entropy Generation Minimization*; CRC Press: Boca Raton, FL, USA, 1995.
6. Wu, F.; Wu, C.; Guo, F.; Li, Q.; Chen, L. Optimization of a thermoacoustic engine with a complex heat transfer exponent. *Entropy* **2003**, *5*, 444–451.
7. Chen, L.; Zheng, T.; Sun, F.; Wu, C. Optimal cooling load and COP relationship of a four-heat-reservoir endoreversible absorption refrigeration cycle. *Entropy* **2004**, *6*, 316–326.
8. Zheng, T.; Chen, L.; Sun, F.; Wu, C. Effect of heat leak and finite thermal capacity on the optimal configuration of a two-heat-reservoir heat engine for another linear heat transfer law. *Entropy* **2003**, *5*, 519–530.
9. Ladino-Luna, D. On optimization of a non-endorreversible Curzon-Ahlborn cycle. *Entropy* **2007**, *9*, 186–197.
10. Ladino-Luna, D. Van der Waals gas as working substance in a Curzon and Ahlborn-Novikov engine. *Entropy* **2005**, *7*, 108–121.
11. Feidt, M. Optimal thermodynamics new upperbounds. *Entropy* **2009**, *11*, 529–547.
12. Bejan, A. Theory of heat transfer-irreversible power plants. *Int. J. Heat Mass Tran.* **1988**, *31*, 1211–1219.
13. Chen, L.; Sun, F.; Wu, C. Influence of internal heat leak on the power *versus* efficiency characteristics of heat engines. *Energ. Convers. Manag.* **1997**, *38*, 1501–1507.
14. Moukalled, F.; Nuwayhid, R.Y.; Noueihed, N. The efficiency of endoreversible heat engines with heat leak. *Int. J. Energ. Res.* **1995**, *19*, 377–389.
15. Howe, J.P. The maximum power, heat demand and efficiency of a heat engine operating in steady state at less than Carnot efficiency. *Energy* **1982**, *7*, 401–402.
16. Wu, C.; Kiang, R.L. Finite-time thermodynamic analysis of a Carnot engine with internal irreversibility. *Energy* **1992**, *17*, 1173–1178.

17. Chen, L.; Sun, F.; Wu, C. A Generalized of real engines and its performance. *J. Energ. Inst.* **1996**, *69*, 214–222.

18. Chen, L.; Sun, F.; Wu, C. Effect of heat transfer law on the performance of a generalized irreversible Carnot engine. *J. Phys. Appl. Phys.* **1999**, *32*, 99.

19. Zhou, S.; Chen, L.; Sun, F.; Wu, C. Optimal performance of a generalized irreversible Carnot-engine. *Appl. Energ.* **2005**, *81*, 376–387.

20. Chen, L.; Li, J.; Sun, F. Generalized irreversible heat-engine experiencing a complex heat-transfer law. *Appl. Energ.* **2008**, *85*, 52–60.

21. Santillán, M.; Maya, G.; Angulo-Brown, F. Local stability analysis of and endoreversible Curzon-Ahlborn-Novikov engine working in a maximum-power like regime. *J. Phys. Appl. Phys.* **2001**, *34*, 2068–2072.

22. Guzman-Vargas, L.; Reyes-Ramirez, I.; Sánchez, N. The effect of heat transfer laws and thermal conductances on the local stability of an endoreversible heat engine. *J. Phys. Appl. Phys.* **2005**, *38*, 1282–1291.

23. Chimal-Eguía, J.C.; Barranco-Jiménez, M.A.; Angulo-Brown, F. Stability analysis of an endoreversible heat engine working with Stefan-Boltzmann heat transfer law working in a maximum power like regime. *Open Syst. Inform. Dynam.* **2006**, *13*, 43–53.

24. Santillán, M.; Mackey, M.C. Dynamic stability *versus* thermodynamic performance in a simple model for a Brownian motor. *Phys. Rev. E* **2008**, *78*, 061122.

25. Angulo-Brown, F. An ecological optimization criterion for finite-time heat engines. *J. Appl. Phys.* **1991**, *69*, 7465–7469.

26. Zhu, X.; Chen, L.; Sun, F.; Wu, C. The ecological optimisation of a generalised irreversible Carnot engine for a generalised heat transfer law. *Int. J. Ambient Energ.* **2003**, *24*, 189–194.

27. Chen, L.; Zhou, J.; Sun, F.; Wu, C. Ecological optimization for generalized irreversible Carnot engines. *Appl. Energ.* **2004**, *77*, 327–338.

28. Zhu, X.; Chen, L.; Sun, F.; Wu, C. Effect of heat transfer law on the ecological optimization of a generalized irreversible Carnot engine. *Open Syst. Inform. Dynam.* **2005**, *12*, 249–260.

29. Chen, L.; Zhu, X.; Sun, F.; Wu, C. Exergy-based ecological optimization of linear phenomenological heat-transfer law irreversible Carnot-engines. *Appl. Energ.* **2006**, *83*, 573–582.

30. Chen, L.; Zhang, W.; Sun, F. Power, efficiency, entropy-generation rate and ecological optimization for a class of generalized irreversible universal heat-engine cycles. *Appl. Energ.* **2007**, *84*, 512–525.

31. Ding, Z.; Chen, L.; Sun, F. Ecological optimization of energy selective electron (ESE) heat engine. *Appl. Math. Model.* **2011**, *35*, 276–284.

32. Yilmaz, T. A new performance criterion for heat engines: Efficient power. *J. Energ. Inst.* **2006**, *79*, 38–41.

33. Paéz-Hernández, R.; Angulo-Brown, F.; Santillán, M. Dynamic robustness and thermodynamic optimization in a non-endoreversible Curzon-Ahlborn engine. *J. Non-Equilib. Thermodyn.* **2006**, *31*, 173–188.

34. Arias-Hernández, L.; de Parga, G.A.; Angulo-Brown, F. On some nonendoreversible engine models with nonlinear heat transfer laws. *Open Syst. Inform. Dynam.* **2003**, *10*, 351–375.

35. Bejan, A. *Shape and Structure, from Engineering to Nature*; Cambridge University Press: Cambridge, UK, 2000.

36. Strogatz, S.H. *Nonlinear Dynamics and Chaos*; Westview Press: Mishawaka, IN, USA, 2000.

37. McDonald, N. *Biological Delay Systems: Linear Stability Theory*; Cambridge University Press: Cambridge, UK, 2008.